



# Assessment of Landslide Susceptibility using Weight of Evidence and Frequency Ratio Model in Shahpur Valley, Eastern Hindu Kush

<sup>1</sup>\*Ghani Rahman, <sup>2</sup>Atta Ur Rahman, <sup>3</sup>Alam Sher Bacha, <sup>4</sup>Shakeel Mahmood,

<sup>5</sup>Muhammad Farhan Ul Moazzam, <sup>5</sup>\*Byung Gul Lee

<sup>1</sup>Department of Geography, University of Gujrat, Pakistan

<sup>2</sup>Department of Geography, University of Peshawar, Pakistan

<sup>3</sup>National Center of Excellence in Geology, University of Peshawar, Pakistan

<sup>4</sup>Government College University, Lahore, Pakistan

<sup>5</sup>Department of Civil Engineering, College of Ocean Sciences, Jeju National University, South Korea

Corresponding author: [ghanigeo@gmail.com](mailto:ghanigeo@gmail.com) [leebg@jejunu.ac.kr](mailto:leebg@jejunu.ac.kr)

## Abstract

This study assessing the landslide susceptibility using Weight of Evidence (WoE) and Frequency Ratio (FR) model in Shahpur valley, situated in the eastern Hindu Kush. Here, landslide is a recurrent phenomenon that disrupts natural environment and cause huge property damages as well as incurs human losses every year. These damages are expected to increase due to high rate of deforestation in the region, population growth, agricultural expansion and infrastructural development on the fragile slopes. Initially, landslide inventory map was prepared from SPOT5 satellite image and were verified from frequent visits in the field. Seven landslide contributing factors including surface geology, fault lines, slope aspect and gradient, land use, proximity to roads and stream were selected. To analyze the relationship of landslide occurrence with these causative factors, WoE and FR models were used. Based on WoE and FR model landslide susceptibility zonation maps were prepared and were reclassified into very low to very high landslide susceptible zones. Finally, the resultant maps of landslide susceptibility were authenticated using success rate curve and prediction rate curve approach to validate the models.

**Keywords:** Landslide Susceptibility, Weight of Evidence, Frequency Ratio, Success rate curve, Prediction rate curve

## 1. Introduction

Globally, the frequency of geological and hydro-meteorological disasters is increased in the last two decades with devastating consequences (Rahman et al. 2017). Landslide is among the geological hazards that cause damages to human life, their property and infrastructure (Jehan & Ahmad 2006). The Hindu Kush-Himalayan (HKH) is young mountain system where landslides, avalanches, floods and earthquakes are very common (A. Rahman & Shaw, 2014; G. Rahman, Rahman, Samiullah, et al., 2017). In this region landsliding is a recurrent phenomenon and mostly been initiated by seismic activity or prolong rainfall (Kamp et al., 2010a; Regmi et al., 2014; G. Rahman, Rahman, & Collins, 2017). The frequent landslide events have been causing damages to



property, infrastructure and sometimes led to human losses. Kanungo et al. (2009) reported that the global share of landslides was five percent among all the natural hazards during 1990-2005 and tend to increase in future because of seismic activities, increasing rainfall intensities and anthropogenic activities on the fragile slopes (Pareek et al., 2010; Conforti et al., 2014; G. Rahman, Rahman, & Collins, 2017).

Landsliding is one of the complex geomorphic process (Nandi & Shakoor, 2010; Allen et al., 2011) mainly triggered by area geology, seismicity, drainage pattern, land cover, gradient and rainfall (Sudmeier-Rieux et al., 2012; G. Rahman, Rahman, Samiullah, et al., 2017). The occurrence of landslides has significant relationship with the slope gradient, aspect, vegetation cover and soil thickness of the slope (Sengupta et al., 2010; Rahman et al. 2011). Prolong rainfall in mountainous areas with fragile slope also increases probabilities of the landslide occurrence. The seismic activities and lithology are other important factors affecting the slope stability (C. Van Westen et al., 2010; A. Rahman et al., 2011). Similarly anthropogenic activities in terms of road construction, expansion of human settlement, deforestation and expansion of agricultural activities on fragile slope further intensifies the landslide susceptibility (Rahman et al. 2017).

The landslides occur throughout the world particularly in certain hotspots (Nadim et al., 2006). Many studies have been conducted to explore the impacts of landslides on human lives, property and infrastructure. A diminutive attention has been given to landslide impacts on the natural environment (Schuster & Highland, 2007). Similarly, attention has been paid to the role of landslides in disturbance of ecological system. The environmental effects caused by landslides are changes in agricultural activities, changes to natural ecosystems, changes in river morphology because of landslide dams (Nakamura et al., 2000). Other effects included sedimentation in river channels and flash flood due to breaching of landslide dams. Landslides also disturbs the natural habitat of certain endanger species in susceptible zone. The landslide events also effects biodiversity of the affected area, therefore strict forest preservation measures are highly required to reduce environmental damage (Geertsema & Pojar, 2007).

Landslide susceptibility is basically the geo-spatial probability of slope failure. The landslides occurrence depends on the presence of some geo-environmental factors (Guzzetti et al., 2005). During past decade, numerous scientific studies including Lee, (2004), Chen and Wang, (2007), Kavzoglu et al., (2014), Bourenane et al., (2016), Ding et al., (2017) and G. Rahman, Rahman, Samiullah, et al., (2017) have been conducted regarding the fragile mountains and established a wide range of empirical approaches for analyzing landslide susceptibility to identify the extent of potentially susceptible landslide areas. Quantitative, semi-quantitative and qualitative techniques including



70 statistical and deterministic approaches has been used in various studies to assess landslide  
 71 susceptibility or hazard zones(C. J. Van Westen et al., 2008). The landslide indices use the semi-  
 72 quantitative, quantitative and qualitative methods for identification of areas having similar  
 73 characteristics with respect to geological and geomorphological settings of the landslide prone areas  
 74 (Kouli et al., 2010). Qualitative methodologies use rating procedure, indigenous knowledge and  
 75 weighting procedures forming bases for semi-quantitative methods. However, quantitative methods  
 76 used statistical techniques to find out the relationship between causal factors and landslide  
 77 events(Ayalew & Yamagishi, 2005).

78 The spatial probability of landslides can be predicted by applying various quantitative  
 79 methodologies like frequency ratio, information value, weight of evidence, fuzzy neural network,  
 80 logistic regression and many others. These methods depend on inventory of past landslides and  
 81 thematic maps of landslide causative factors(Hussin et al., 2016). In recent years, geospatial  
 82 technology is widely applied in studies regarding landslide susceptibility mapping, risk identification  
 83 and management (Akbar & Ha, 2011). Geospatial technology provides a framework for mapping the  
 84 past landslide events and combine the landslide causative factors for producing landslide  
 85 susceptibility map and therefore it has become an integral part of landslide susceptibility zonation  
 86 (LSZ).

87 The HKH is an active seismic region and hence most of the landslides have also been initiated  
 88 by seismic activity (Kamp et al., 2010b). Developmental work is usually affected by the frequently  
 89 occurring phenomena of landsliding in the HKH region. It is therefore, a dire need of time to identify  
 90 the landslide prone areas that will not only minimize the risk of landsliding in future but will also  
 91 provide base for the future planning as well. In present study the landslide susceptibility mapping is  
 92 based on frequency ratio and weight of evidence model to develop landslide susceptibility maps of  
 93 Shahpur valley, HKH region.

## 94 **2. The Study Area**

95 The study area, Shahpur valley lies in the Hindu Raj Mountains. These mountains are  
 96 considered as the offshoot of Hindu Kush mountain system (Dichter, 1967). Moving from north to  
 97 south the height of these Hindu Kush Mountains tends to decreases. The latitudinal extent of the  
 98 valley is 34° 52' 31" to 35° 9' 35" while longitudinal extent is 72° 40' 10" to 72° 48' 44" as shown in  
 99 the Figure 1. The total area of Shahpur valley is approximately 259 square kilometers. Climatically,  
 100 Shahpur valley is the part of moist temperate zone. The valley receives heavy rainfall during summer  
 101 season from monsoon, while in winter at higher altitudes mostly precipitation occurs in the form of



heavy snowfall. Climate of the valley remain mild to warm in summer while temperature decrease to  
 chill cold in winter season throughout the valley (G. Rahman et al., 2019).

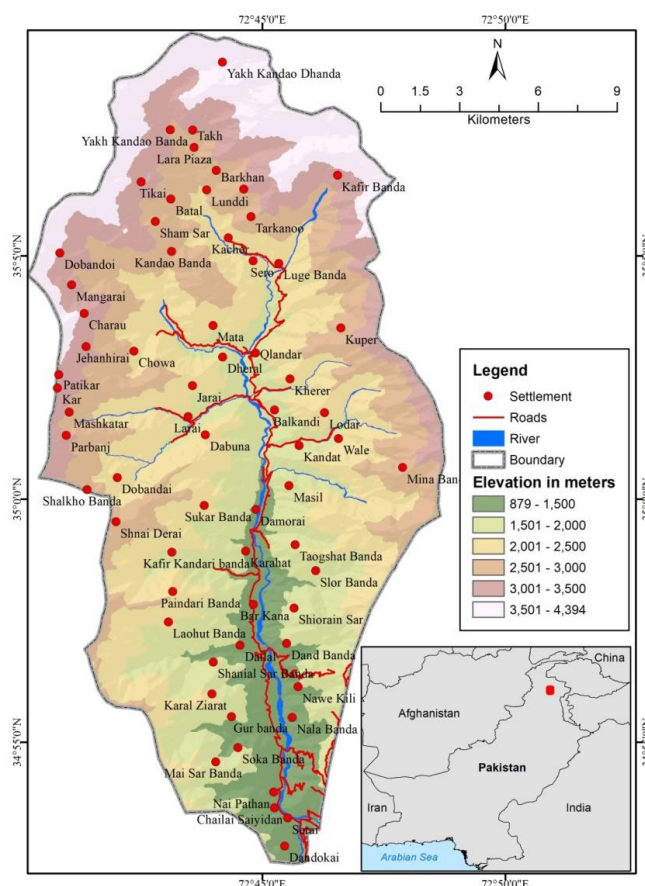


Figure 1: Digital Elevation Map of Shahpur valley

HKH region came into existence due to the collision of Eurasian and Indian plate during the Cretaceous and Mio-Pliocene epoch. As a result of this collision these mountains are still continuously rising at a rate of 4 to 5 mm/year (Jehan & Ahmad, 2006). There is high altitudinal variation of 3600 meters in just 259 square km area (Figure 1). The valley has steep slope in the upper part while it became gentle in the lower reach of the valley. The valley is drained by a stream known as Khan Khwar. The study area consist of young mountain system that have immature geology and is prone to landsliding phenomena which often results considerable property damages and human losses almost every. The probability of these damages is expected to increase further as a result of anthropogenic activities like deforestation, overgrazing, agricultural activities and



115 development of infrastructure in this area. Population growth has posed more pressure on the fragile  
 116 slopes and has made it more vulnerable for landsliding.

117

### 118 **3. Methods and Material**

119 In the eastern Hindu Kush region, Shahpur valley was selected for detailed analysis to grasp  
 120 the governing landslide causative factors, which frequently trigger landsliding. The data from both  
 121 primary and secondary data sources were used to achieve the objectives of the study (Figure 2). The  
 122 past landslide sites were identified and mapped on 2.5m resolution SPOT image of April 2013. A  
 123 thorough field study was conducted to confirm the landslide sites on the ground and identify the  
 124 landslide triggering factors with local community knowledge. Seven triggering factors namely  
 125 surface geology, proximity to fault line, slope gradient and aspect, land use/ land cover, nearness to  
 126 road and streams were identified.

127 Data regarding landslide triggering factors were acquired including the surface geology and  
 128 tectonics from geological map of North Pakistan. The administrative boundaries and settlement  
 129 shape-files was prepared from topographic sheets (RF 1:50,000) obtained from survey of Pakistan.  
 130 Spatial features of roads network was acquired from the office of Communication and Works  
 131 Department, Peshawar. Land use/land cover map was obtained after applying supervised  
 132 classification on SPOT satellite image using ArcGIS 10.2. ASTERGDEM having 30m was used for  
 133 extracting slope angle, slope aspect and hydrology of the study area. Furthermore, a detailed field  
 134 survey was conducted to validate the sites of already activated and potentially active landslide area.

135 GIS and Remote Sensing have been used for the preparation of spatial databases and  
 136 landslides inventory map. Weight of evidence and frequency ratio model analysis is a bivariate  
 137 statistical methodology in which the importance of each factor or combined factors is individually  
 138 analyzed with respect to spatial distribution of existing landslides. The assumption in both models is  
 139 that the factors which influenced the incidence of landslides in the past will be the same to trigger  
 140 new landslides in future.

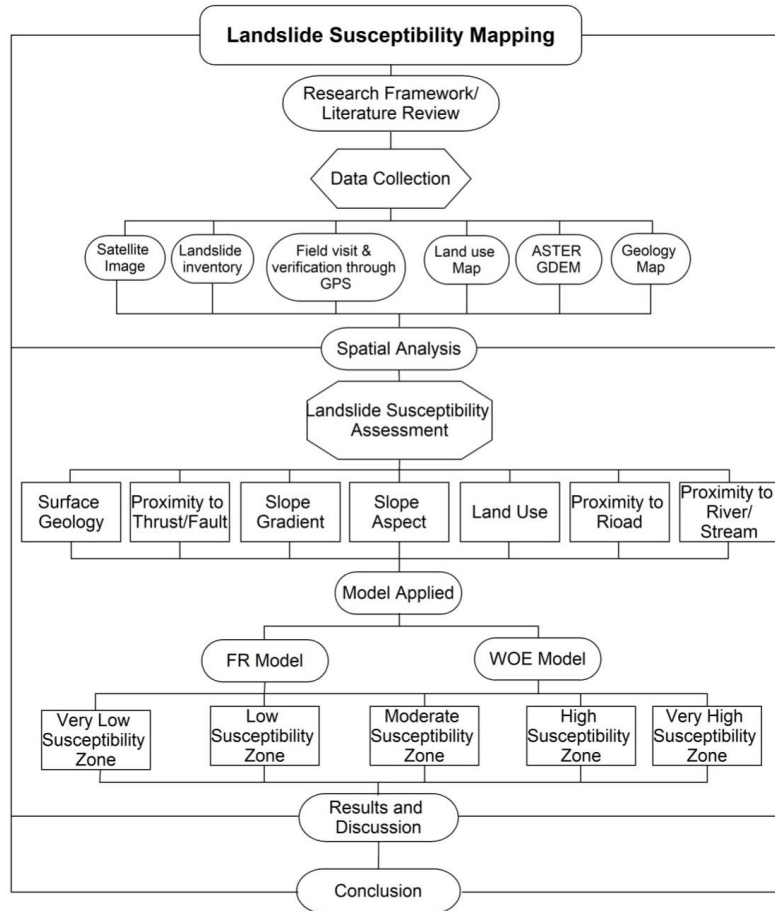


Figure 2: Research Model

### 3.1 Weight of Evidence Model

Weight of evidence model (Bonham-Carter et al., 1989; Bonham-Carter, 1994) is based on Eq. 1 and Eq. 2:

$$W^+ = \ln \frac{P\left(\frac{B}{D}\right)}{P\left(\frac{\bar{B}}{\bar{D}}\right)} \quad (1)$$

$$W^- = \ln \frac{P\left(\frac{\bar{B}}{\bar{D}}\right)}{P\left(\frac{B}{D}\right)} \quad (2)$$

In the above equations,  $P$  is the probability while  $\ln$  is the natural log.  $B$  and  $\bar{B}$  respectively represent the presence and absence of potential landslide evidence factor. Likewise,  $D$  and  $\bar{D}$  is the presence and absence of landslide respectively. For the calculation of weight of each causative



factors contributing in landslide occurrence Eq.3 and Eq.4 have been used after (C. Van Westen et al., 2003).

$$W^+ = \ln \left\{ \left( \frac{N_{pix1}}{N_{pix1} + N_{pix2}} \right) / \left( \frac{N_{pix3}}{N_{pix3} + N_{pix4}} \right) \right\} \quad (\text{Eq.3})$$

$$W^- = \ln \left\{ \left( \frac{N_{pix3}}{N_{pix1} + N_{pix2}} \right) / \left( \frac{N_{pix4}}{N_{pix3} + N_{pix4}} \right) \right\} \quad (\text{Eq.4})$$

Where the  $N_{pix1}$  is the number of pixels express the existence of both landslide contributing factor and landslides;  $N_{pix2}$  represent the presence of landslide and absence of landslide contributing factor. While  $N_{pix3}$  represent the presence of landslide contributing factor and absence of landslide. Similarly,  $N_{pix4}$  represent the absence of both landslide and landslide contributing factors. Final weight expressed with  $W^c$  was calculated using Eq.5:

$$W^c = (W^+) - (W^-) \quad (\text{Eq.5})$$

Where,  $W^c$  is the difference of  $W^+$  and  $W^-$ . This elucidates the spatial relationship of all landslide contributing factors and landslide.

### 3.2 Frequency Ratio Model

To analyze the effect of landslide contributing factors on the occurrence of landsliding was also examined through frequency ratio model. It is a ratio of landslides occurred area with respect to the total study area, and is also the proportion of the landslide occurrence probabilities to a non-occurrence for a given attribute (Bonham-Carter, 1994; Lee & Talib, 2005). In frequency ratio model, a statistical value for each class of a factor map using the Eq.6:

$$FR = \frac{N_{pix(Si)} / N_{pix(Ni)}}{\sum N_{pix(Si)} / \sum N_{pix(Ni)}} \quad (\text{Eq.6})$$

Where,  $N_{pix(Si)}$  is the number of landslide pixels containing class  $i$ ,  $N_{pix(Ni)}$  is the total number of pixels of class  $i$ ,  $\sum N_{pix(Si)}$  is total number of landslide pixels in the entire study area, whereas  $\sum N_{pix(Ni)}$  is the total number of pixels of the entire study area.

### 3.3 Landslide Susceptibility Index (LSI)

LSI for both, frequency ratio and weight of evidence model was generated by combining the landslide causative/ contributing factors in GIS based on the  $W^c$  and  $FR$  values for overlay analysis using the Eq.7:

$$LSI = \sum W^c, LSI = \sum FR \quad (\text{Eq.7})$$



179 Where  $\sum W^c$  is the total derived weight of weight of evidence model and  $\sum FR$  is the total derived  
 180 weight of frequency ratio model.

## 181 **4. Results and Discussion**

182 In this paper frequency ratio and weight of evidence models are used with aim to determine  
 183 and geo-visualize the landslide susceptibility with resultant map is susceptibility zonation that has  
 184 been extensively applied in many parts of the world for landslides risk reduction(Shahabi et al.,  
 185 2015).

### 186 **4.1 Inventory of Landslides in Shahpur Valley**

187 The past landslides sites were marked on multi-spectral SPOT satellite image of April 2013. These  
 188 sites were verified in through series of field visits. About three hundred landslides of varying sizes  
 189 were marked on the satellite image and verified from field investigation in the study area (G. Rahman  
 190 et al., 2019) (Figure 3). This landslide inventory was randomly divided into two groups, group one  
 191 was taken as training landslides (80%) and the second group was taken as validation landslides  
 192 (20%). These landslides were then rasterized to find out the number of pixels in every class of a  
 193 factor map for calculation of frequency ratio and weight of evidence model values.

### 194 **4.2 Landslide Contributing/ causative factors**

195 Landsliding is a natural phenomenon and its occurrence is determined by variety of causative factors.  
 196 In this study, surface lithology/geology, stream buffer for assessing impacts of stream proximity, land  
 197 cover, slope aspect, slope gradient, fault line impacts and impacts of road network were selected as  
 198 landslides contributing factors (Figure 4). WoE and FRM statistical models based on correlation of  
 199 past landslide and causative factors were used to define the weight of each class of every factor map.  
 200 In WoE model the positive weight ( $W^+$ ), negative weight ( $W^-$ ) and contrast weight ( $W^c$ ) while for  
 201 FR model the frequency ratio were calculated for each class of a contributing factor map (Table 1).

202



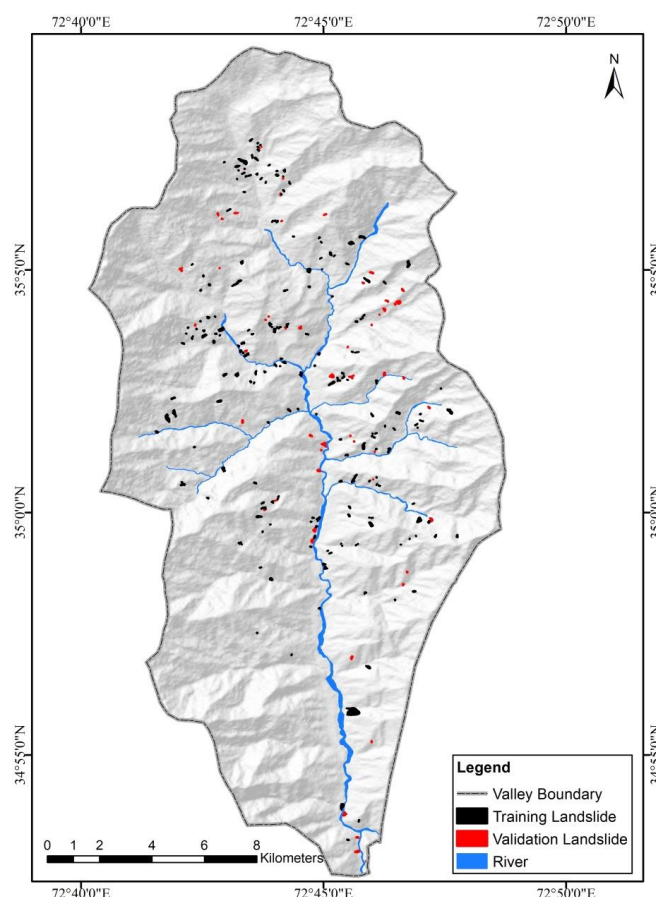


Figure 3: Shahpur valley, Landslide inventory and distribution of past landslides

#### 4.2.1 Surface Geology

To assess the relationship of surface geology and landslide occurrence in Shahpur valley, surface geology was taken as a causative factor and its relationship were assessed using WoE and FRM. Surface geology types are shown in Figure 4g. The highest positive  $W^c$  weight was found in Darwaza Sar Potassic Granite Gneiss (0.71) and Alluvium (0.59). These both classes have very positive correlation with landslides using WoE model. Alluvium in this region is of quaternary period and is brought by Indus river and its tributaries derived from the Kohistan island arc terrane (Baig, 1990). Similar results were found in FR values. The highest negative correlation was in geology class Jijal Ultramafics having  $W^c$  value -3.64 and FR 0.03 (Table 1).

#### 4.2.2 Fault Line

The occurrence of landslides has a strong correlation with fault lines (Korup, 2004; G. Rahman, Rahman, & Collins, 2017). Fault lines existence at high slope gradient provides favorable



217 settings for slope failure. There is a complex tectonic structure in the study area and is considered as  
 218 causal factor in slope instability. It is evident from the analysis that the tectonic structures have strong  
 219 correlation with landslide occurrence. The highest positive  $W^c$  value (1.56) was found in the area of  
 220 buffer zone 0-250 meters followed by 251-500 meters buffer zone and the lowest  $W^c$  was in area of  
 221 greater than 1000 meters according to WoE model. Similar results was found in frequency ratio  
 222 model, the highest FR value (2.87) was in the buffer zone of 0-250 meters and the lowest was in area  
 223 of greater than 1000 meters area.

224 **Table 1.** Shahpur valley, calculated weight of each class of causative factors

Classes	$N_{pix}$ (Si)	%age of $N_{pix}$ (Si)	$N_{pix}$ (Ni)	%age of $N_{pix}$ (Ni)	$W^+$	$W^-$	$W^c$	FR
<b>Surface Geology</b>								
Alluvium	1499	18.52	290137	11.20	0.51	-0.09	0.59	1.65
Greenschist Melange	806	9.96	165892	6.40	0.44	-0.04	0.48	1.56
Jabrai Granite Gneiss	903	11.16	497979	19.22	-0.54	0.10	-0.64	0.58
Alpuraicalc-mica-garnet schist	990	12.23	235014	9.07	0.30	-0.04	0.34	1.35
Karora Group	967	11.95	501955	19.37	-0.48	0.09	-0.57	0.62
Besham Group	1436	17.74	441986	17.06	0.04	-0.01	0.05	1.04
Manglaur Formation	1218	15.05	378895	14.62	0.03	-0.01	0.03	1.03
Darwaza Sar Potassic Granite Gneiss	271	3.35	43693	1.69	0.69	-0.02	0.71	1.99
Jijal Ultramafics	3	0.04	35939	1.39	-3.63	0.01	-3.64	0.03
<b>Fault Line Buffer (m)</b>								
0 – 250	4018	49.65	448304	17.30	1.06	-0.50	1.56	2.87
251 – 500	2325	28.73	409420	15.80	0.60	-0.17	0.77	1.82
501 – 1000	760	9.39	676634	26.11	-1.02	0.20	-1.23	0.36
> 1000	990	12.23	1057133	40.79	-1.21	0.40	-1.60	0.30
<b>Slope Gradient</b>								
0-5°	91	1.12	67722	2.61	-0.85	0.02	-0.86	0.43
6-15°	514	6.35	261492	10.09	-0.46	0.04	-0.50	0.63
16-30°	2138	26.42	668931	25.81	0.02	-0.01	0.03	1.02
31-45°	4847	59.89	1366442	52.73	0.13	-0.16	0.29	1.14
> 46°	503	6.22	226903	8.76	-0.34	0.03	-0.37	0.71
<b>Slope Aspect</b>								
Flat	1	0.01	1004	0.04	-1.14	0.00	-1.14	0.32
North	503	6.22	214667	8.28	-0.29	0.02	-0.31	0.75
Northeast	531	6.56	284530	10.98	-0.52	0.05	-0.56	0.60
East	1444	17.84	387999	14.97	0.18	-0.03	0.21	1.19
Southeast	881	10.89	395492	15.26	-0.34	0.05	-0.39	0.71
South	1775	21.93	366954	14.16	0.44	-0.10	0.53	1.55
Southwest	1135	14.02	356943	13.77	0.02	0.00	0.02	1.02
West	819	10.12	317383	12.25	-0.19	0.02	-0.22	0.83
Northwest	1004	12.41	266520	10.28	0.19	-0.02	0.21	1.21



Land Cover								
Range Land	2762	34.13	847632	32.71	0.04	-0.02	0.06	1.04
Forest	2621	32.39	1036194	39.98	-0.21	0.12	-0.33	0.81
Glacier and Snow	108	1.33	111086	4.29	-1.17	0.03	-1.20	0.31
Agriculture Land	2100	25.95	416925	16.09	0.48	-0.13	0.61	1.61
Settlement	48	0.59	37521	1.45	-0.89	0.01	-0.90	0.41
Barren Land	87	1.08	87880	3.39	-1.15	0.02	-1.17	0.32
Stream/torrent	367	4.53	54252	2.09	0.78	-0.03	0.80	2.17
Road Buffer (m)								
0-100	769	9.50	130869	5.05	0.63	-0.05	0.68	1.88
101-200	541	6.68	103117	3.98	0.52	-0.03	0.55	1.68
201-300	591	7.30	92441	3.57	0.72	-0.04	0.76	2.05
301-400	141	1.74	85731	3.31	-0.64	0.02	-0.66	0.53
> 400	6051	74.77	2179333	84.10	-0.12	0.46	-0.58	0.89
Stream Buffer (m)								
0-100	1918	23.70	294902	11.38	0.74	-0.15	0.89	2.08
101-200	1555	19.21	265711	10.25	0.63	-0.11	0.74	1.87
201-300	1021	12.62	255277	9.85	0.25	-0.03	0.28	1.28
301-400	799	9.87	247979	9.57	0.03	0.00	0.03	1.03
401-500	395	4.88	238952	9.22	-0.64	0.05	-0.68	0.53
>500	2405	29.72	1288669	49.73	-0.52	0.34	-0.85	0.60

### 4.2.3 Slope Gradient

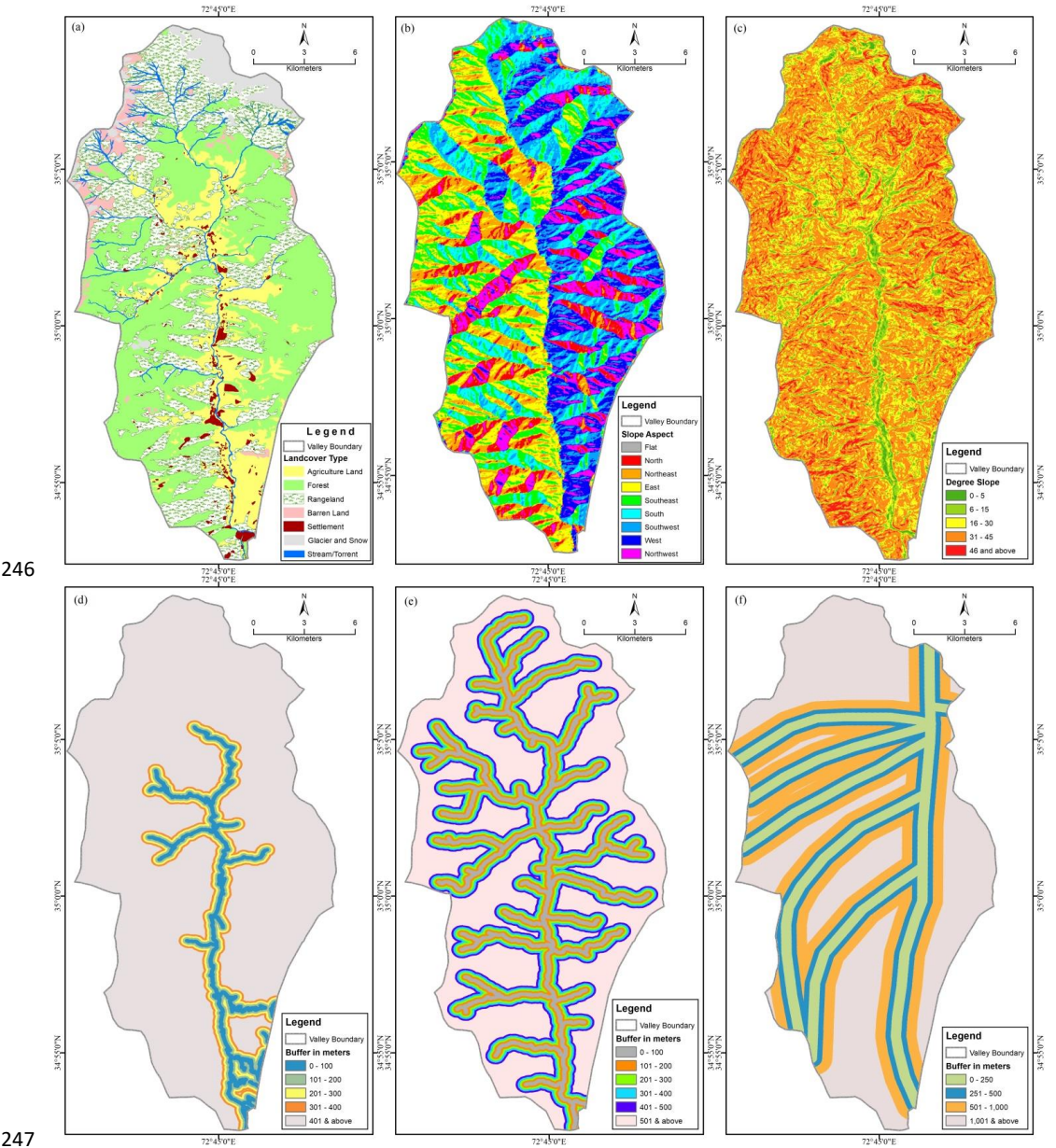
Slope gradient affects the population distribution, their activities and distribution of natural resources. Likewise, landslide distribution also has a close association with slope gradient and act as a controlling factor in slope failure. Slope gradient has direct relation with slope failure and the chances of landslide incidence escalate with increase in slope gradient. It was observed during field visits that the high landslide density areas were on the slope along the road and stream where lateral cutting was dominant factor. Map of the slope gradient for the study area was generated from AsterGDEM having 30 meters spatial resolution in GIS (Figure 4c). The analysis of both WoE and FRM shows that the role of 31-45 degree slope is higher in slope failure as the highest  $W^c$  value (0.29) and FR value (1.14) was found in this class of slope gradient (Table 1). While the slope gradient 0-5 and 6-15 degree class has negative correlation with landslide.

### 4.2.4 Slope Aspect

Slope aspect does not have a direct impact on landslide occurrence, but indirectly accelerate the landslide process. The sunlight intensity and duration, amount of rainfall and moisture holding capacity and distribution of vegetation all are affected by slope direction. The analysis reveals that the south facing slope has very strong positive correlation with landslide as the value of  $W^c$  (0.53)



243 and FR (1.55) is higher in this class followed by northwest  $W^c$ (0.21) and FR (1.21) facing slope  
244 (Table 1). In the study area, high landslides in south facing slopes may be due to its high exposition  
245 to sunlight and receiving ample amount of rainfall as of windward side.



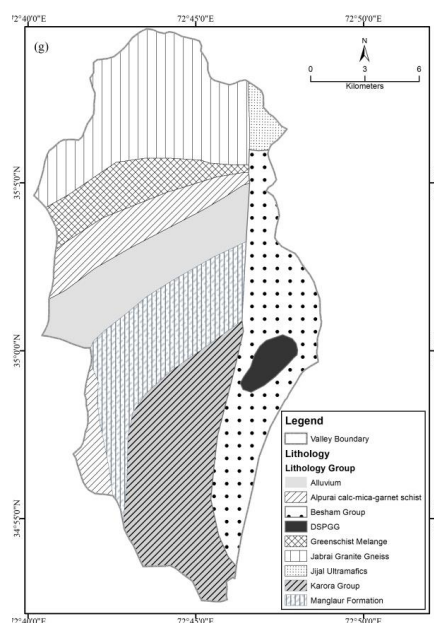


**Fig. 4.** Shahpur valley: (a) Land use map; (b) Slope aspect; (c) Slope gradient; (d) proximity to road; (e) Proximity to stream; (f) Proximity to fault lines; (g) Surface geology

#### 4.2.5 Land Use/ Land Cover

The forest cover protect the mountainous slope from weathering and mass wasting processes as the roots hold the underneath soil and keep the slope stable. Increasing population growth has increase the demand of wood and land for food has disturbed the slope of almost all the mountainous region of the world and have led to slope instability. Land cover of Shahpur valley was developed from the SPOT satellite of image (Figure 4a). Analyzing the influence of land use/ land cover on landslide, statistical weight for each class of the land use was calculated using WoE and frequency ratio model. The highest weight of both WoE ( $W^c = 0.80$ ) and FR (2.17) was found for stream/torrent class. This was because in the study area the stream/torrent has high lateral erosion and thus initiates new slides. The second high positive correlation was of agriculture land with landslide. In the study area forest cover are mostly cleared for agriculture activities. Agriculture practice is on terrace field which also make the slope susceptible to landslide. It was found from the analysis that barren land has negative correlation with landslide as in the study area the land was barren because of presence of hard rock masses which does not support any vegetation in the higher slopes.



#### 266 4.2.6 Proximity to Road

267 The road constructions often disturb the slope and expedite the weathering and mass wasting process  
 268 thus increase the probability of landslide occurrence. It also provides means of accessibility and  
 269 accelerates the process of deforestation. In the current study, proximity to road is used as a causative  
 270 factor of landslide. The results show high positive correlation with road proximity up to 300 meter.  
 271 The highest  $W^c$  value (0.68) and FR (1.88) was found in 0-100 meters road proximity. This elucidate  
 272 that the slope near to road have more probability to slope failure.

#### 273 4.2.7 Proximity to Stream/torrent

274 In order to examine the relationship of stream/torrent on landslide, WoE and frequency ratio  
 275 statistical models were applied. It was found from the analysis that both WoE and FRM have higher  
 276 value near the stream that indicates high probability in this region. The highest  $W^c$  (0.89) and FR  
 277 value (2.08) were found in the proximity of 0-100 meters (Table 1). The results show that the region  
 278 up to 400 meters of proximity to stream shows the positive correlation toward the landslide  
 279 probability. The highest negative correlation was found in the region of greater than greater than 500  
 280 meters of stream.

#### 281 4.3 Landslide Susceptibility Zonation

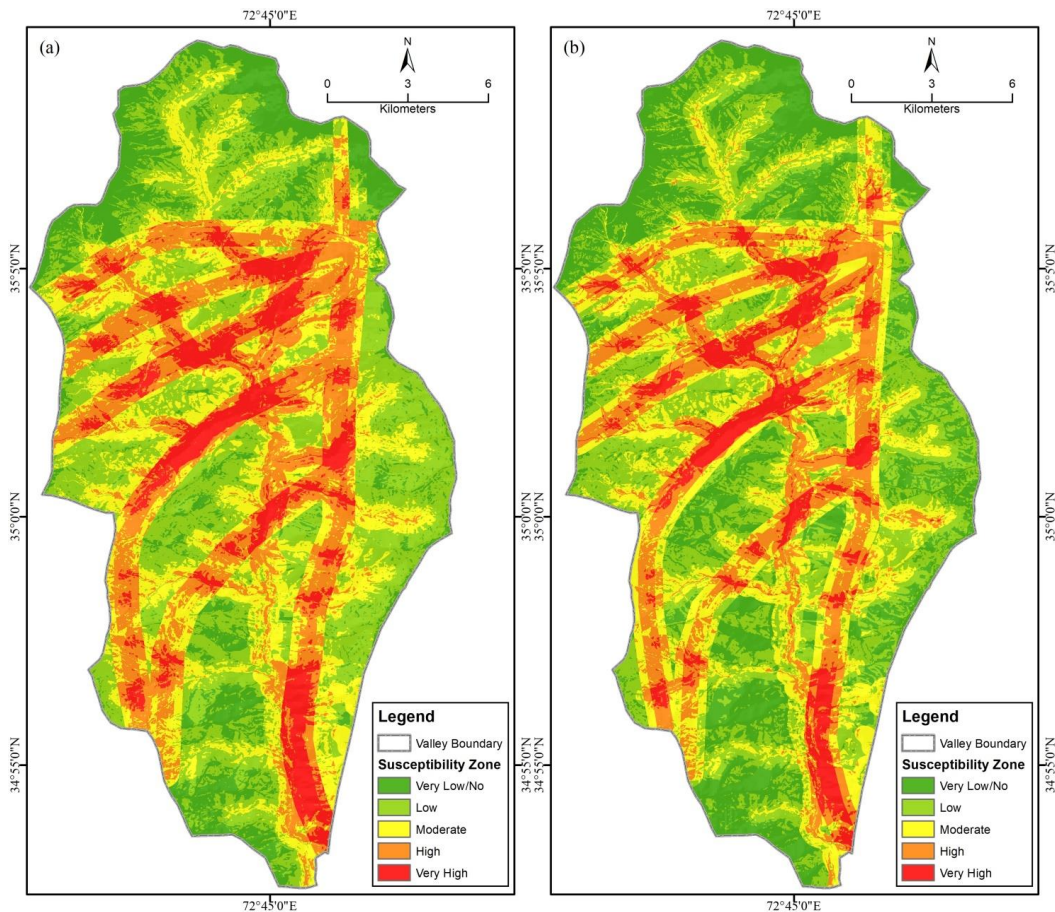
282 Landslide is the common menace to the property, human lives and infrastructure in Shahpur  
 283 valley. For its mitigation the first utmost important step is to identify high susceptible landslide areas.  
 284 LSZ map divide the region into very low to very high susceptible zone according to their  
 285 susceptibility based on integration of landslide causal factors. GIS provides framework for  
 286 integration of different landslide causal factors to produce LSZ map. To minimize subjectivity,  
 287 quantitative weight to each class of factor maps was applied based WoE and FR models for  
 288 generation of LSZ map of Shahpur valley. The LSZ map was created based on both WoE and FR  
 289 models by summing all the relative weight of each class of factor maps using following expressions:

$$290 \quad LSI = \sum W^c \quad (8)$$

$$291 \quad LSI = \sum FR \quad (9)$$

292 Where  $\sum W^c$  is the total derived weight of each class of the factor maps for WoE model, while  
 293  $\sum FR$  is the sum of the derived weight of each class of the factor map of frequency ratio model. In  
 294 both cases the higher the value of LSI, greater would be the probability of landslides incident. Based  
 295 on LSI, the study area was divided into zones of Very high to very low Susceptibility.





296  
297 **Fig. 5.** Shahpur valley, (a) landslide susceptibility zones based on WoE; (b) landslide susceptibility  
298 zones based on FR  
299

300 **4.4 Validation of Landslide Susceptibility Map**

301 The landslide susceptibility map was validated using success rate curve based on training  
302 landslide that were 80% of the total landslide inventory and prediction rate curve using validation  
303 landslides that were 20% of the total landslide inventory. The success rate curve and prediction rate  
304 curve elucidates the accuracy of WoE and FRM for selected causative factors to landslide  
305 occurrences. Success rate curve and prediction rate curve was calculated using the LSI values ranging  
306 from highly susceptible to very low susceptible class and overlaid with the existing layer of landslide  
307 area through geo-statistical tool in GIS. Cumulative percentages for both susceptibility class and  
308 landslide area were calculated and susceptibility class was plot on x-axis and landslide area on y-axis  
309 to generate both success rate curve and prediction rate curve. Both success rate curve and prediction



rate curve have steep curve which indicates significant result for both WoE and FR models. Both the susceptibility maps prepared based on WoE and FR models were validated using area under (AUC) technique. It is a quantitative measurement of success rate and predictive rates of the landslide susceptibility map. The AUC for WoE model was 87.92% for success rate curve and 79.19% for prediction rate curve. Likewise, the FR model result shows that the AUC was 90.92% for success rate curve and 84.38% for prediction rate curve. In the current study, both the models are having high accuracy and both model are suitable for landslide susceptibility studies in the Hindu Kush region.

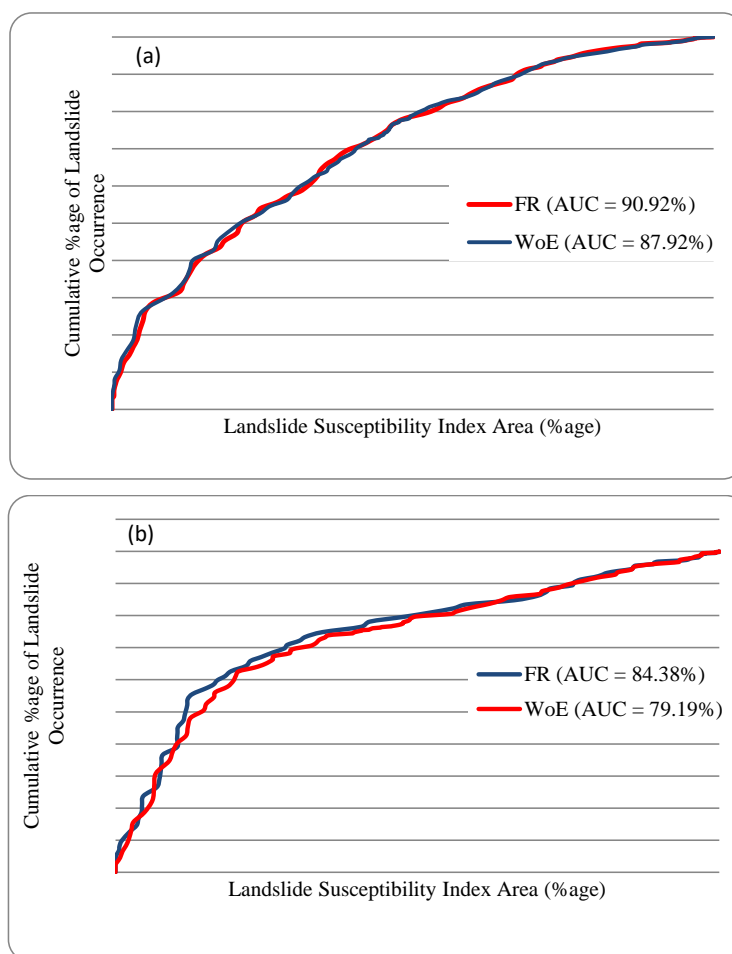


**Fig. 6.** Shahpur valley, (a) Success rate curve, (b) Prediction rate curve; showing the prediction capability of WoE and FR models





## 5 Conclusion

In the current study frequency ratio and weight of evidence models were applied to develop landslide susceptibility map. Initially, past landslides were identified from SPOT satellite image and consecutive field visits and plotted on map. Landslide causative factors that were identified from literature review including surface lithology, fault lines, land cover, slope gradient and aspect, distance from streams and roads. The maps of these factors were prepared for susceptibility analysis. The roles of each class of these factor maps in landslide occurrence were analyzed and assigned weights were calculated by implementing Bayesian probability models i.e. weight of evidence and frequency ratio. The required susceptibility maps were generated using  $\sum W^c$  and  $\sum FR$  values through overlay analysis in GIS.

The maps of landslide susceptibility were prepared based on both models and then validated using success rate curve and prediction rate curve. It is further concluded that in Shahpur valley, the results of frequency ratio model proved better than the weight of evidence model for landslide susceptibility studies in the Hindu Kush region. This study can assist the disaster management authorities to develop location specific mitigation measures for landslide hazards to avoid loss of life and damages to infrastructure in future. The study conclude that landslide hazard in the region may have negative impacts on agricultural activities, natural ecosystem, on river morphology, human lives and infrastructure in the study area. In this regard proper land use planning and strict forest preservation measures are highly required to reduce environmental damage.

## Conflict of Interest

All authors have no conflict of interest.

## References

- Akbar, T. A., & Ha, S. R. (2011). Landslide hazard zoning along Himalayan Kaghan Valley of Pakistan—by integration of GPS, GIS, and remote sensing technology. *Landslides*, 8(4), 527-540.
- Allen, S. K., Cox, S. C., & Owens, I. F. (2011). Rock avalanches and other landslides in the central Southern Alps of New Zealand: a regional study considering possible climate change impacts. *Landslides*, 8(1), 33-48.
- Ayalew, L., & Yamagishi, H. (2005). The application of GIS-based logistic regression for landslide susceptibility mapping in the Kakuda-Yahiko Mountains, Central Japan. *Geomorphology*, 65(1), 15-31.
- Baig, M. S. (1990). Structure and geochronology of Pre-Himalayan and Himalayan orogenic events in the Northwest Himalayan, Pakistan, with special reference to the Besham area. (PhD), *Oregon State University*.
- Bonham-Carter, G. F. (1994). Geographic information systems for geoscientists-modeling with GIS. *Computer methods in the geoscientists*, 13, 398.



- 359 Bonham-Carter, G. F., Agterberg, F. P., & Wright, D. F. (1989). Weights of evidence modeling: a new approach  
 360 to mapping mineral potential. *Statistical applications in the earth sciences*, 171-183.
- 361 Bourenane, H., Guettouche, M. S., Bouhadad, Y., & Braham, M. (2016). Landslide hazard mapping in the  
 362 Constantine city, Northeast Algeria using frequency ratio, weighting factor, logistic regression,  
 363 weights of evidence, and analytical hierarchy process methods. *Arabian Journal of Geosciences*, 9(2),  
 364 154.
- 365 Chen, Z., & Wang, J. (2007). Landslide hazard mapping using logistic regression model in Mackenzie Valley,  
 366 Canada. *Natural hazards*, 42(1), 75-89.
- 367 Conforti, M., Pascale, S., Robustelli, G., & Sdao, F. (2014). Evaluation of prediction capability of the artificial  
 368 neural networks for mapping landslide susceptibility in the Turbolo River catchment (northern  
 369 Calabria, Italy). *Catena*, 113, 236-250.
- 370 Dichter, D. (1967). *The North-West Frontier of West Pakistan: A Study in Regional Geography*: Clarendon  
 371 Press.
- 372 Ding, Q., Chen, W., & Hong, H. (2017). Application of frequency ratio, weights of evidence and evidential  
 373 belief function models in landslide susceptibility mapping. *Geocarto international*, 32(6), 619-639.
- 374 Geertsema, M., & Pojar, J. J. (2007). Influence of landslides on biophysical diversity—a perspective from  
 375 British Columbia. *Geomorphology*, 89(1-2), 55-69.
- 376 Guzzetti, F., Reichenbach, P., Cardinali, M., Galli, M., & Ardizzone, F. (2005). Landslide hazard assessment in  
 377 the Staffora basin, northern Italian Apennines. *Geomorphology*, 72, 272-299.
- 378 Hussin, H. Y., Zumpano, V., Reichenbach, P., Sterlacchini, S., Micu, M., van Westen, C., & Bălteanu, D. (2016).  
 379 Different landslide sampling strategies in a grid-based bi-variate statistical susceptibility model.  
 380 *Geomorphology*, 253, 508-523. doi:https://doi.org/10.1016/j.geomorph.2015.10.030
- 381 Jehan, N., & Ahmad, I. (2006). Petrochemistry of asbestos bearing rocks from Skhakot-Qila Ultramafic  
 382 Complex northern Pakistan. *JHES*, 39, 75-83.
- 383 Kamp, U., Owen, L. A., Growley, B. J., & Khattak, G. A. (2010a). Back analysis of landslide susceptibility  
 384 zonation mapping for the 2005 Kashmir earthquake: an assessment of the reliability of susceptibility  
 385 zoning maps. *Natural hazards*, 54(1), 1-25.
- 386 Kamp, U., Owen, L. A., Growley, B. J., & Khattak, G. A. (2010b). Back analysis of landslide susceptibility  
 387 zonation mapping for the 2005 Kashmir earthquake: an assessment of the reliability of susceptibility  
 388 zoning maps. *Natural Hazards*, 54(1), 1-25.
- 389 Kavzoglu, T., Sahin, E. K., & Colkesen, I. (2014). Landslide susceptibility mapping using GIS-based multi-criteria  
 390 decision analysis, support vector machines, and logistic regression. *Landslides*, 11(3), 425-439.
- 391 Korup, O. (2004). Landslide-induced river channel avulsions in mountain catchments of southwest New  
 392 Zealand. *Geomorphology*, 63(1-2), 57-80.
- 393 Kouli, M., Loupasakis, C., Soupios, P., & Vallianatos, F. (2010). Landslide hazard zonation in high risk areas of  
 394 Rethymno Prefecture, Crete Island, Greece. *Natural Hazards*, 52(3), 599-621.
- 395 Lee, S. (2004). Application of likelihood ratio and logistic regression models to landslide susceptibility  
 396 mapping using GIS. *Environmental Management*, 34(2), 223-232.
- 397 Lee, S., & Talib, J. A. (2005). Probabilistic landslide susceptibility and factor effect analysis. *Environmental*  
 398 *Geology*, 47(7), 982-990.
- 399 Nadim, F., Kjekstad, O., Peduzzi, P., Herold, C., & Jaedicke, C. (2006). Global landslide and avalanche  
 400 hotspots. *Landslides*, 3(2), 159-173.
- 401 Nakamura, F., Swanson, F. J., & Wondzell, S. M. (2000). Disturbance regimes of stream and riparian  
 402 systems—a disturbance-cascade perspective. *Hydrological Processes*, 14(16-17), 2849-2860.
- 403 Nandi, A., & Shakoor, A. (2010). A GIS-based landslide susceptibility evaluation using bivariate and  
 404 multivariate statistical analyses. *ENG GEOL*, 110(1), 11-20.
- 405 Pareek, N., Sharma, M. L., & Arora, M. K. (2010). Impact of seismic factors on landslide susceptibility  
 406 zonation: a case study in part of Indian Himalayas. *Landslides*, 7(2), 191-201.
- 407 Rahman, A., Khan, A. N., Collins, A. E., & Qazi, F. (2011). Causes and extent of environmental impacts of  
 408 landslide hazard in the Himalayan region: a case study of Murree, Pakistan. *Natural Hazards*, 57(2),  
 409 413-434.



- 410 Rahman, A., & Shaw, R. (2014). Floods in the Hindu Kush Region: causes and socio-economic aspects.  
 411 *Mountain hazards and disaster risk reduction. Springer, Tokyo*, 33-52.
- 412 Rahman, G., Rahman, A.-U., & Collins, A. (2017). Geospatial analysis of landslide susceptibility and zonation in  
 413 shahpur valley, eastern hindu kush using frequency ratio model. *Proceedings of the Pakistan*  
 414 *Academy of Sciences*, 54(3), 149-163.
- 415 Rahman, G., Rahman, A.-u., Ullah, S., Miandad, M., & Collins, A. E. (2019). Spatial analysis of landslide  
 416 susceptibility using failure rate approach in the Hindu Kush region, Pakistan. *Journal of Earth System*  
 417 *Science*, 128(3), 59.
- 418 Rahman, G., Rahman, A., Samiullah, & Collins, A. (2017). Geospatial analysis of landslide susceptibility and  
 419 zonation in shahpur valley, eastern hindu kush using frequency ratio model. *Proceedings of the*  
 420 *Pakistan Academy of Sciences*, 54(3), 149-163.
- 421 Regmi, A. D., Devkota, K. C., Yoshida, K., Pradhan, B., Pourghasemi, H. R., Kumamoto, T., & Akgun, A. (2014).  
 422 Application of frequency ratio, statistical index, and weights-of-evidence models and their  
 423 comparison in landslide susceptibility mapping in Central Nepal Himalaya. *Arabian Journal of*  
 424 *Geosciences*, 7(2), 725-742.
- 425 Schuster, R. L., & Highland, L. M. (2007). Overview of the effects of mass wasting on the natural environment.  
 426 *Environmental & Engineering Geoscience*, 13(1), 25-44.
- 427 Sengupta, A., Gupta, S., & Anbarasu, K. (2010). Rainfall thresholds for the initiation of landslide at Lanta Khola  
 428 in north Sikkim, India. *Natural Hazards*, 52(1), 31-42.
- 429 Shahabi, H., Hashim, M., & Ahmad, B. B. (2015). Remote sensing and GIS-based landslide susceptibility  
 430 mapping using frequency ratio, logistic regression, and fuzzy logic methods at the central Zab basin,  
 431 Iran. *Environmental Earth Sciences*, 73(12), 8647-8668.
- 432 Sudmeier-Rieux, K., Jaquet, S., Derron, M.-H., Jaboyedoff, M., & Devkota, S. (2012). A case study of coping  
 433 strategies and landslides in two villages of Central-Eastern Nepal. *APPL GEOGR*, 32(2), 680-690.
- 434 Van Westen, C., Quan Luna, B., Vargas Franco, R., Malet, J., Jaboyedoff, M., Horton, P., & Kappes, M. (2010).  
 435 Development of training materials on the use of geo-information for multi-hazard risk assessment in  
 436 a mountainous environment. Paper presented at the *Proceedings of the Mountain Risks International*  
 437 *Conference, Firenze, Italy*.
- 438 Van Westen, C., Rengers, N., & Soeters, R. (2003). Use of geomorphological information in indirect landslide  
 439 susceptibility assessment. *Natural hazards*, 30(3), 399-419.
- 440 Van Westen, C. J., Castellanos, E., & Kuriakose, S. L. (2008). Spatial data for landslide susceptibility, hazard,  
 441 and vulnerability assessment: an overview. *ENG GEOL*, 102(3), 112-131.

442